



## OPEN D-serine and D-alanine supplementation protects against chronic kidney disease

Yusuke Nakade<sup>1,2</sup>, Yasunori Iwata<sup>1</sup>✉, Tadashi Toyama<sup>1</sup>, Taku Kobayashi<sup>1</sup>, Masashi Mita<sup>3</sup>, Yuta Yamamura<sup>1</sup>, Megumi Oshima<sup>1</sup>, Toshiaki Tokumaru<sup>1,4</sup>, Shinji Kitajima<sup>1</sup>, Miho Shimizu<sup>1</sup>, Norihiko Sakai<sup>1</sup> & Takashi Wada<sup>1</sup>

Novel therapeutic targets for renal protection are imperative due to the escalating prevalence of end-stage kidney disease despite existing treatments for chronic kidney disease (CKD). We explored the reno-protective effects of D-serine and D-alanine, which have previously demonstrated efficacy in acute kidney injury against CKD. Female and male 5/6-nephrectomy mice were used as CKD models, receiving 20 mM D-serine or D-alanine supplementation, and their survival rates, renal function, and transcriptomic changes were examined. The proliferation of human tubular epithelial cells supplemented with D-serine or D-alanine was evaluated *in vitro*. A prospective cohort study involving 14 patients was conducted to examine the association between increased blood D-serine or D-alanine levels and long-term renal function decline. D-serine or D-alanine supplementation improved survival rates and renal function in female 5/6-nephrectomy mice. D-alanine supplementation was associated with the upregulation of mitochondrial pathway-related genes. Long-term supplementation (500 days) in normal mice did not induce nephrotoxicity, and promoted tubular epithelial cell proliferation. Although a trend toward a slower decline in eGFR was observed in patients with higher D-alanine levels, this association was limited and does not indicate a causal relationship. Further studies involving D-Ala interventions in patients with CKD are needed to confirm these findings.

**Keywords** Chronic kidney disease, D-alanine, D-serine, Supplementation, Therapeutic option

The number of patients with chronic kidney disease (CKD) and those undergoing hemodialysis (HD) is increasing. In 2017, the estimated global prevalence of CKD was 9.1%, representing a 29.3% increase since 1990<sup>1</sup>. Nutrition therapy is the first step in CKD management and is pivotal in protecting renal function and reducing the risk of complications, including cardiovascular disease. Specifically, regulating sodium, protein, potassium, and phosphorus intake has been shown to slow disease progression and alleviate symptoms<sup>2-4</sup>. Furthermore, while reno-protective drugs such as renin-angiotensin system inhibitors and sodium-glucose cotransporter 2 inhibitors reduce the risk of kidney dysfunction progression<sup>5-9</sup>, novel therapeutic options are required to address the residual risks of end-stage kidney disease. In this context, we focused on D-amino acids (AAs) as a novel dietary and therapeutic candidate for CKD. We have previously reported the reno-protective effects of D-serine (D-Ser) and D-alanine (D-Ala) in a mouse model of acute kidney injury (AKI) induced by ischemia/reperfusion (I/R). The D-Ser and D-Ala levels reportedly increase in the blood of humans and mice with AKI<sup>10-12</sup>. D-Ser showed anti-inflammatory effects in tubular I/R injury and promoted tubular epithelial cell (TEC) proliferation<sup>10</sup>. The kidneys of mice treated with D-Ser show increased TEC proliferation due to the activation of the mammalian target of rapamycin (mTOR)-related pathway<sup>11</sup>. D-Ala also increased TEC proliferation and anti-renal fibrosis by inhibiting the production of mitochondrial reactive oxygen species (ROS)<sup>12</sup>. Therefore, increased D-Ser and D-Ala blood levels might reduce renal damage in AKI cases.

In addition to AKI, D-Ser and D-Ala blood levels are elevated in patients with CKD and those undergoing hemodialysis (HD)<sup>13</sup>. Based on the reno-protective effects of D-Ser and D-Ala observed in AKI models, we hypothesized that these D-amino acids (D-AAAs) could potentially aid in mitigating CKD progression. To test this hypothesis, we assessed long-term renal function in patients treated with risperidone, an inhibitor of the

<sup>1</sup>Department of Nephrology and Rheumatology, Kanazawa University, 13-1 Takara-machi, Kanazawa 920-8641, Japan. <sup>2</sup>Department of Clinical Laboratory, Kanazawa University Hospital, 13-1 Takara-machi, Kanazawa 920-8641, Japan. <sup>3</sup>KAGAMI Co., Ltd., 7-18 Saitobaohiruzu Centre 308, Ibaragi-shi 567-0085, Osaka, Japan. <sup>4</sup>Department of Nutrition, Kanazawa University Hospital, 13-1 Takara-machi, Kanazawa 920-8641, Japan. ✉email: iwatay@staff.kanazawa-u.ac.jp

D-AA degrading enzyme. Patients taking risperidone exhibited higher blood concentrations of D-Ser and D-Ala compared to non-treated patients and exhibited a slower decline in the estimated glomerular filtration rate (eGFR)<sup>14</sup>. Further evidence is provided by a study that evaluated eGFR in healthy participants before and after D-Ala supplementation. Post-supplementation, both eGFR and blood D-Ala levels increased, returning to baseline levels once supplementation was discontinued<sup>15</sup>. These findings suggest that elevated D-Ser and D-Ala blood levels might contribute to renal function maintenance over the long term, suggesting their potential relevance in CKD management.

In this study, we aimed to determine whether long-term administration of D-Ser or D-Ala in a CKD mouse model improves kidney function and pathology, leading to an extended lifespan. Additionally, the associations between the blood D-Ser or D-Ala levels and renal prognosis were evaluated in patients with CKD.

## Results

### Survival rate of 5/6-Nx mice receiving D-Ser or D-Ala orally

Blood levels of D-Ser and D-Ala were significantly elevated in 5/6 nephrectomized (5/6-Nx) mice treated with D-Ser or D-Ala in drinking water compared to non-treated mice (Fig. 1a,b). Conversely, levels of L-AAs such as L-Ser and L-Ala remained unchanged. (Fig. 1c,d). Female 5/6-Nx mice treated with D-Ser or D-Ala in drinking water lived longer than those untreated (log-rank  $p < 0.05$ ) (Fig. 1e,f). Female 5/6-Nx mice treated with D-Ser or D-Ala in drinking water survived almost as long as female sham mice (log-rank  $p > 0.05$ ) (Fig. 1g,h). No significant difference was observed between sham and 5/6-Nx male mice (log-rank  $p = 0.058$ ) (Fig. 1i).

### Renal function of 5/6-Nx mice receiving D-Ser or D-Ala orally

The renal function was assessed to investigate the reno-protective effects of D-Ser or D-Ala in female mice. Female 5/6-Nx mice treated with D-Ser or D-Ala in drinking water had lower plasma blood urea nitrogen (BUN) and Cr levels than those untreated (Fig. 2a,b). Furthermore, the 24-h urine volume from female 5/6-Nx mice treated with D-Ala in drinking water decreased (Fig. 2c). However, the male 5/6-Nx and sham mice showed only slight differences. On day 100, male 5/6-Nx mice treated with D-Ser or D-Ala showed lower plasma BUN levels than those untreated (Fig. 2d). Plasma Cr levels and 24-h urine volume did not differ between male 5/6-Nx mice receiving D-Ser or D-Ala and those untreated (Fig. 2e,f).

Next, we explored whether long-term D-Ser or D-Ala administration could cause kidney dysfunction in mice. Renal function was evaluated in normal mice, and 20 mM D-Ser or D-Ala was administered orally for 500 days. No differences in plasma BUN (Supplemental Fig. S1a) and Cr (Supplemental Fig. S1b) levels and 24-h urine volume (Supplemental Fig. S1c) were found between the mice with/without D-Ser or D-Ala supplementation. Therefore, long-term D-Ser or D-Ala oral administration did not affect renal function.

In female 5/6-Nx mice, the survival rate and renal function improved upon treatment with D-Ser or D-Ala in drinking water compared with those in untreated mice. Therefore, we subsequently focused on female mice and comprehensively examined renal pathology, physical characteristics, and genetic changes.

### Renal pathology of female 5/6-Nx mice treated with D-Ser or D-Ala

Female 5/6-Nx mice treated with D-Ser or D-Ala showed less necrosis and better brush border scores than untreated female 5/6-Nx mice (Fig. 3a–d,i,j). Furthermore, female 5/6-nephrectomy mice treated with D-alanine exhibited less severe renal fibrosis than untreated mice (Fig. 3e–h). Quantitative evaluation using hydroxyproline also showed that female 5/6-Nx mice treated with D-Ala in their drinking water had lower hydroxyproline levels compared to untreated female 5/6-Nx mice (Fig. 3k).

### Physical characteristics of female 5/6-Nx mice receiving D-Ser or D-Ala orally

Next, changes in physical characteristics were evaluated. Female 5/6-Nx mice and D-Ser-treated female 5/6-Nx mice continued to lose weight compared to sham mice. However, the body weight of female 5/6-Nx mice treated with D-Ala did not differ from that of sham mice (Fig. 4a). At 200 days after 5/6-Nx surgery, the 5/6-Nx and D-Ser-treated 5/6-Nx mice were smaller in size compared to the sham mice and showed alopecia. However, female D-Ala-treated 5/6-Nx mice were similar in size to the sham mice; they exhibited no shedding (Fig. 4b). Blood pressure and heart rate showed variations in 5/6-Nx mice compared to sham controls but did not exhibit consistent increases or decreases over time. (Supplemental Fig. 2a,b).

Water consumption increased in 5/6-Nx mice compared to sham controls (Fig. 4c), whereas feed intake remained unchanged (Fig. 4d). No difference was observed in these parameters between 5/6-Nx mice and 5/6-Nx mice that had been administered D-Ala in their drinking water.

### RNA-Seq analysis of kidneys from female 5/6-Nx mice receiving D-Ser or D-Ala orally

Next, we evaluated the effects of D-Ser or D-Ala administration on the kidneys of female 5/6-Nx mice at the gene level to elucidate the reno-protective mechanisms of D-Ser or D-Ala. The expression of 11 of 13,483 genes was altered in D-Ala-supplemented female 5/6-Nx mice, compared with that in untreated female 5/6-Nx mice; nine genes (*Cndp1*, *Mtfr1*, *Bhmt*, *Apool*, *Unc13c*, *Bmp7*, *Lonp1*, *Etv5*, and *Zfp704*) were upregulated, and two (*Herpud1* and *Noct*) were downregulated (Fig. 5a). For D-ser, no genes met the significance threshold of  $q\text{-value} < 0.10$  and  $\text{Log}_2 \text{Fold Change} > 0.5$ . For reference, genes that showed changes when  $q\text{-value} < 0.20$  and  $\text{Log}_2 \text{Fold Change} > 0.5$  are shown. The expression of two of 13,483 genes was altered in D-Ser-supplemented female 5/6-Nx mice, compared with that in untreated female 5/6-Nx mice; *Bhmt* was upregulated, and *Polr1a* was downregulated (Fig. 5b).

The cluster analysis was performed using the 11 genes differentially expressed between untreated and D-Ala-treated female 5/6-Nx mice. Two major clusters were identified (Fig. 5c). We analyzed gene ontology (GO) using the genes differentially expressed upon oral administration of D-Ala. Terms primarily associated with

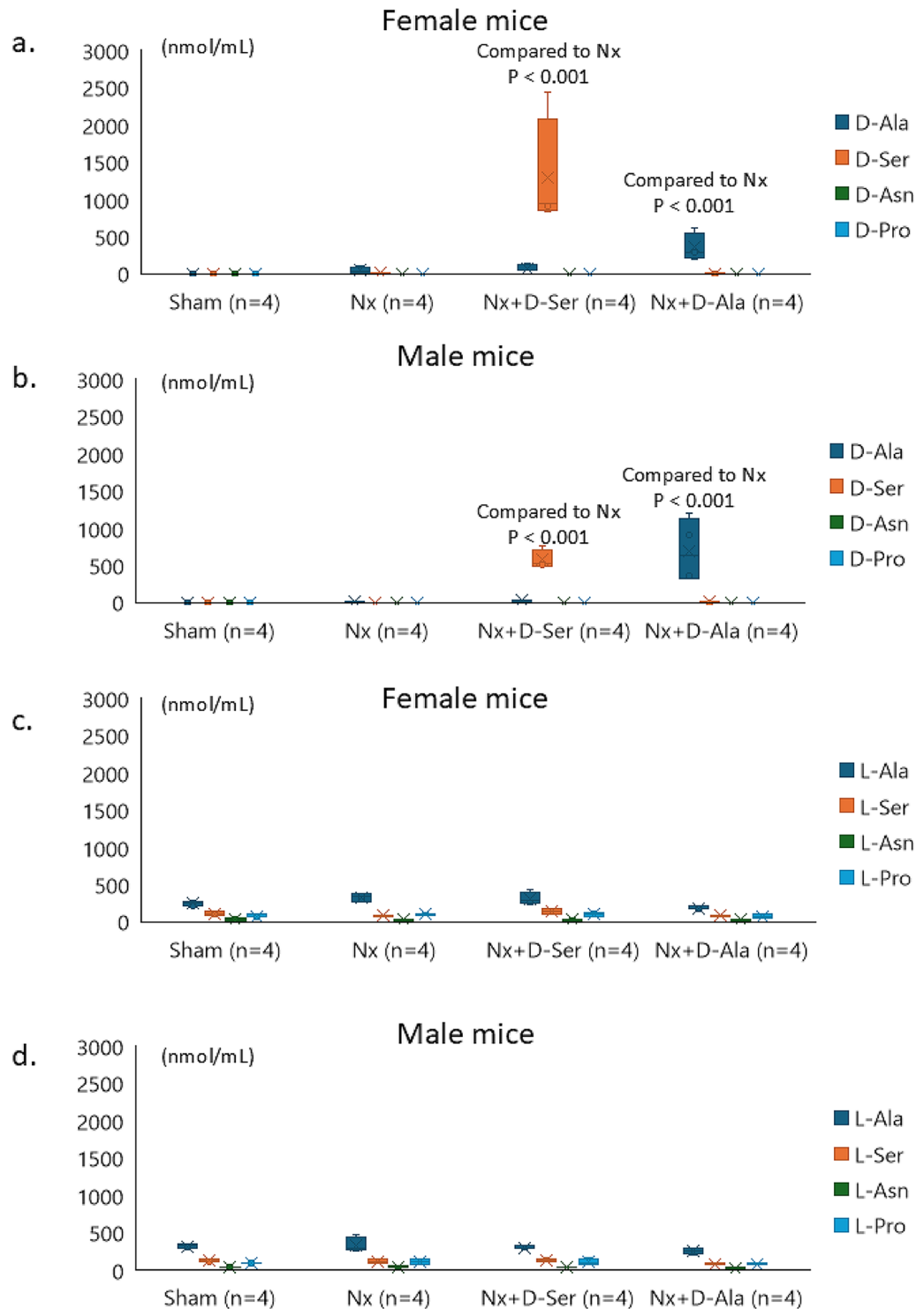


**Fig. 1.** Oral administration of 20 mM D-Ser or D-Ala improves renal function in female 5/6-Nx mice. Plasma Ala, Ser, Asn, and Pro levels were measured in male and female mice (a–d); D-amino acid (ab) and L-amino acid levels (cd) were shown. Survival data of female (e–h) and male mice (i) orally administered D-Ser or D-Ala are shown. Female 5/6-Nx mice treated with D-Ser (e) and D-Ala (f) survived longer than untreated female 5/6-Nx mice ( $p < 0.05$ ). No significant difference was found between the survival time of 5/6-Nx female mice treated with D-Ser (g) and D-Ala (h) and that of sham female mice. Statistical analysis was performed using the Kaplan–Meier method. *Ala* alanine, *Ser* serine, *Asn* asparagine, *Pro* proline, *Nx* nephrectomy.

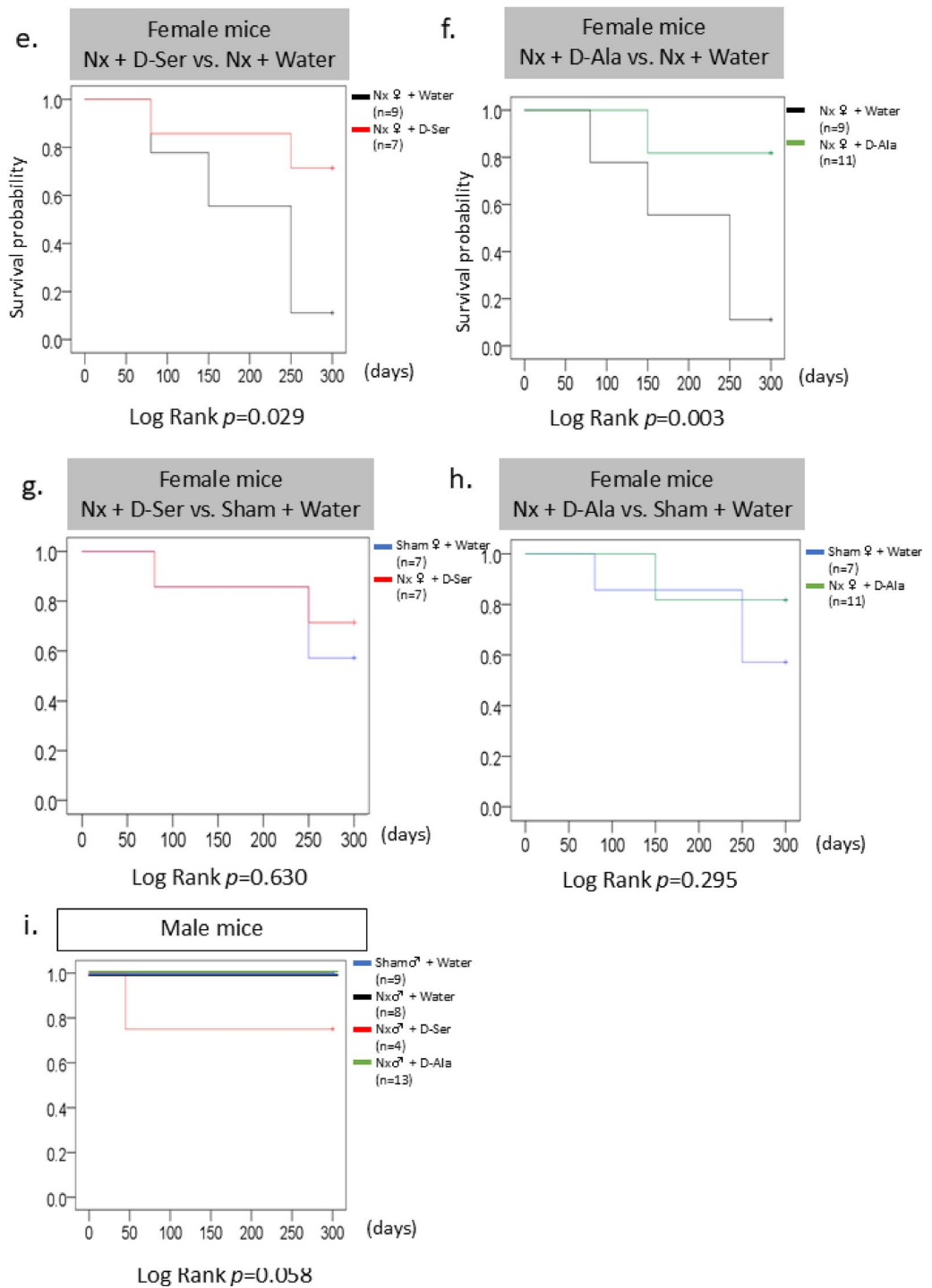
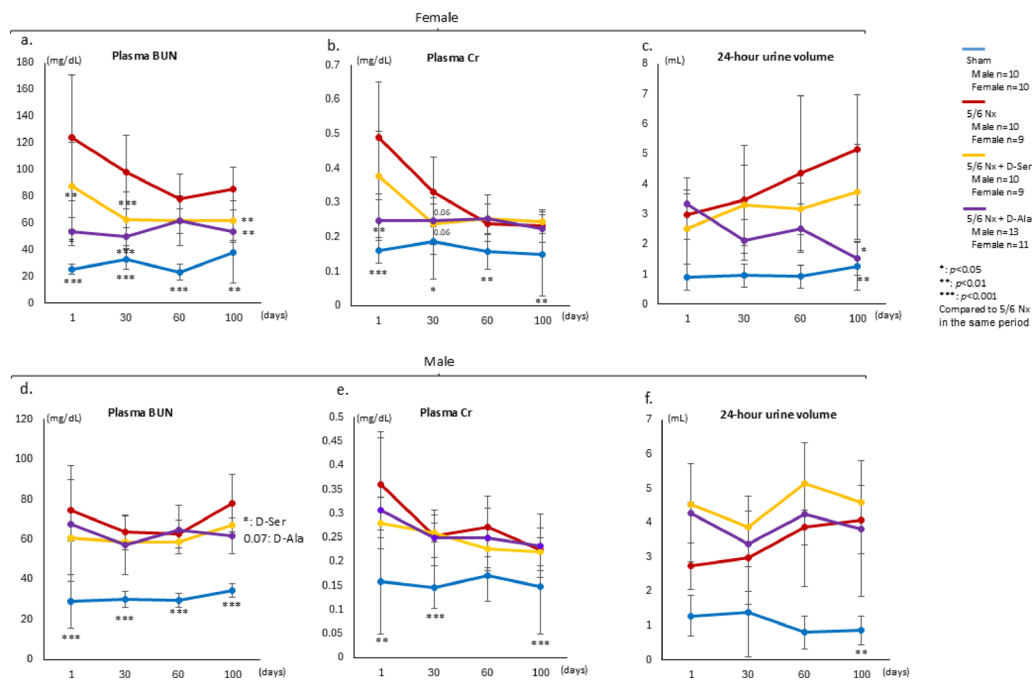


Fig. 1. (continued)

mitochondria were classified into annotation cluster 1 (Fig. 5d). No relevant GO terms were obtained using the genes differentially expressed by oral D-Ser administration (data not shown).

#### Relationship between blood D-AA levels and renal prognosis in patients with CKD

Next, we analyzed the relationship between plasma D-Ala or D-Ser levels and annual eGFR loss in a longitudinal study of human participants. The mean observation period was 31.6 months. At baseline, the plasma D-Ala levels were higher in patients with diabetic kidney disease (DKD) than in healthy volunteers (Fig. 6a). The plasma D/L-Ala levels—corrected for D-AA levels with L-AA levels—were also higher in patients with DKD compared to those in healthy individuals. Plasma D/L-Ser levels were higher in patients with CKD and those with DKD than in healthy volunteers (Fig. 6b).



**Fig. 2.** Oral administration of 20 mM D-Ser or D-Ala improves renal function in female 5/6-Nx mice. Plasma BUN (**a, d**), plasma Cr (**b, e**), and 24-h urine volume (**c, f**) from the sham and 5/6-Nx mice of both sexes were measured. Oral administration of 20 mM D-Ser or D-Ala improved the plasma BUN and Cr levels in female 5/6-Nx mice (**a, b**). Oral administration of 20 mM D-Ala improved 24-h urine volume in female 5/6-Nx mice (**c**). \* $p < 0.05$ , \*\* $p < 0.01$ , \*\*\* $p < 0.001$ , as analysed using a t-test. *BUN* blood urea nitrogen, *Cr* creatinine, *D-Ala* D-alanine, *D-Ser* D-serine, *Nx* nephrectomy.

No association was found between the plasma D-Ala or D-Ser levels and the eGFR slope in patients with CKD (Fig. 6c). Patients with CKD were divided into the DKD and no DKD groups. Figure 6d shows an association between higher plasma D-Ala levels and slower eGFR decline in patients with DKD ( $p < 0.0001$ ). Conversely, there was no significant association between the L-Ser or L-Ala levels and eGFR slopes in patients with DKD (Supplementary Fig. 3). Therefore, patients with DKD and high D-Ala levels were protected from an eGFR decline. Thus, an association between D-Ala levels and eGFR slope was observed in patients with DKD.

### Proliferative effects of D-Ser or D-Ala on human TECS

Then, we examined the effects of D-Ser or D-Ala on the human TEC line HK-2. D-Ser treatment promoted HK-2 proliferation at 10–100  $\mu\text{M}$  and inhibited proliferation at 1,000  $\mu\text{M}$ . D-Ala also promoted HK-2 proliferation at 10–1,000  $\mu\text{M}$  (Supplementary Fig. 4). Therefore, concentrations of approximately 100  $\mu\text{M}$  and 1,000  $\mu\text{M}$  of D-Ser and D-Ala in vitro facilitated cell proliferation without including cytotoxic effects.

### Discussion

D-Ser or D-Ala administration improved renal function and histological outcomes in female 5/6-Nx mice, with treated mice exhibiting higher survival rates than untreated controls. Their renoprotective potential has been demonstrated in previous ischemia-reperfusion injury models, with mitochondrial protection and mTOR activation identified as key mechanisms<sup>10–12</sup>. Given the well-established link between renal function and life expectancy<sup>16</sup>, our findings further support the therapeutic potential of D-Ser or D-Ala in CKD.

In this study, we demonstrated that oral D-Ala administration alleviated kidney injury and performed RNA-seq analysis to elucidate its underlying mechanism. The results confirmed an increase in *Lonp1* expression in D-Ala-treated mice. *Lonp1* is a mitochondrial protease essential for maintaining mitochondrial homeostasis, oxidative stress response, and protein quality control<sup>17</sup>. Reduced *Lonp1* expression has been associated with CKD progression, whereas its overexpression has been shown to mitigate renal injury and mitochondrial dysfunction<sup>18</sup>. Furthermore, pharmacological *Lonp1* activation has been shown to attenuate renal fibrosis and enhance mitochondrial function in CKD<sup>19</sup>. These findings suggest that *Lonp1* upregulation in D-Ala-treated mice is a key mechanism underlying D-Ala's renoprotective effects, likely by enhancing mitochondrial function and reducing oxidative stress.

Additionally, RNA-seq analysis revealed a significant upregulation of *Bmp7* expression in D-Ala-treated mice. *Bmp7* plays a crucial role in kidney development and renal tissue maintenance<sup>20,22,23</sup>. It exerts anti-inflammatory effects by suppressing macrophage infiltration and fibrosis in kidney injury models<sup>21,22,24</sup>. Exogenous *Bmp7* administration has been shown to alleviate renal fibrosis and inflammation in animal models<sup>22,24</sup>. Importantly, *Bmp7* antagonizes TGF- $\beta$  signaling, inhibiting TGF- $\beta$ /Smad3-mediated renal fibrosis through the Smad1/5/8

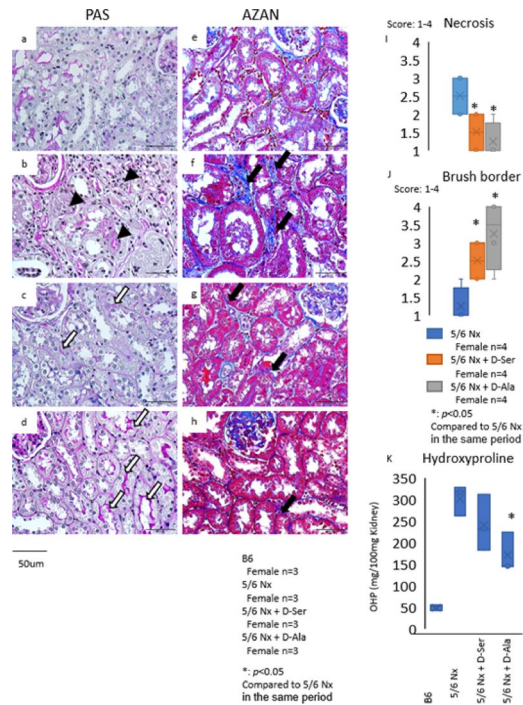


**Fig. 3.** Oral administration of D-Ser or D-Ala improves renal impairment in female 5/6-Nx mice. Results of PAS and azan staining of the kidneys are shown. Sham (a, e), female 5/6-Nx (b, f), orally supplemented with 20 mM D-Ser (c, g), and orally supplemented with D-Ala (d, h) female 5/6-Nx mice. Necrosis score (i), brush border score (j), and hydroxyproline level (k) are shown. Box plots use horizontal lines to indicate the median, 25th, and 75th percentile values. Black arrowheads denote necrosis. Black arrows denote fibrosis. White arrows denote the brush border. \* $p < 0.05$ , as analyzed using a t-test. *D-Ala* D-alanine, *D-Ser* D-serine, *Nx* nephrectomy, *PAS* periodic acid-Schiff.

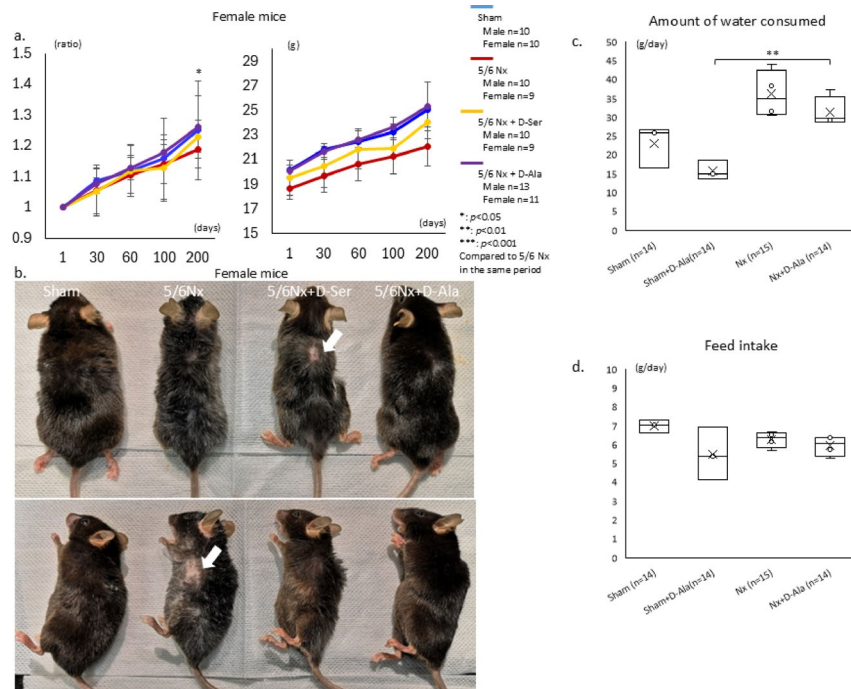


**Fig. 4.** Oral administration of D-Ala prevents weight and hair loss in female 5/6-Nx mice. Weight (a) and appearance (b) of sham and female 5/6-Nx mice. Oral administration of 20 mM D-Ala suppressed female 5/6-Nx mice's weight and hair loss (white arrows). Intake of water (c) and feed (d) by sham and female 5/6-Nx mice. \* $p < 0.05$ , as analyzed using a t-test. *D-Ala* D-alanine, *D-Ser* D-serine, *Nx* nephrectomy.

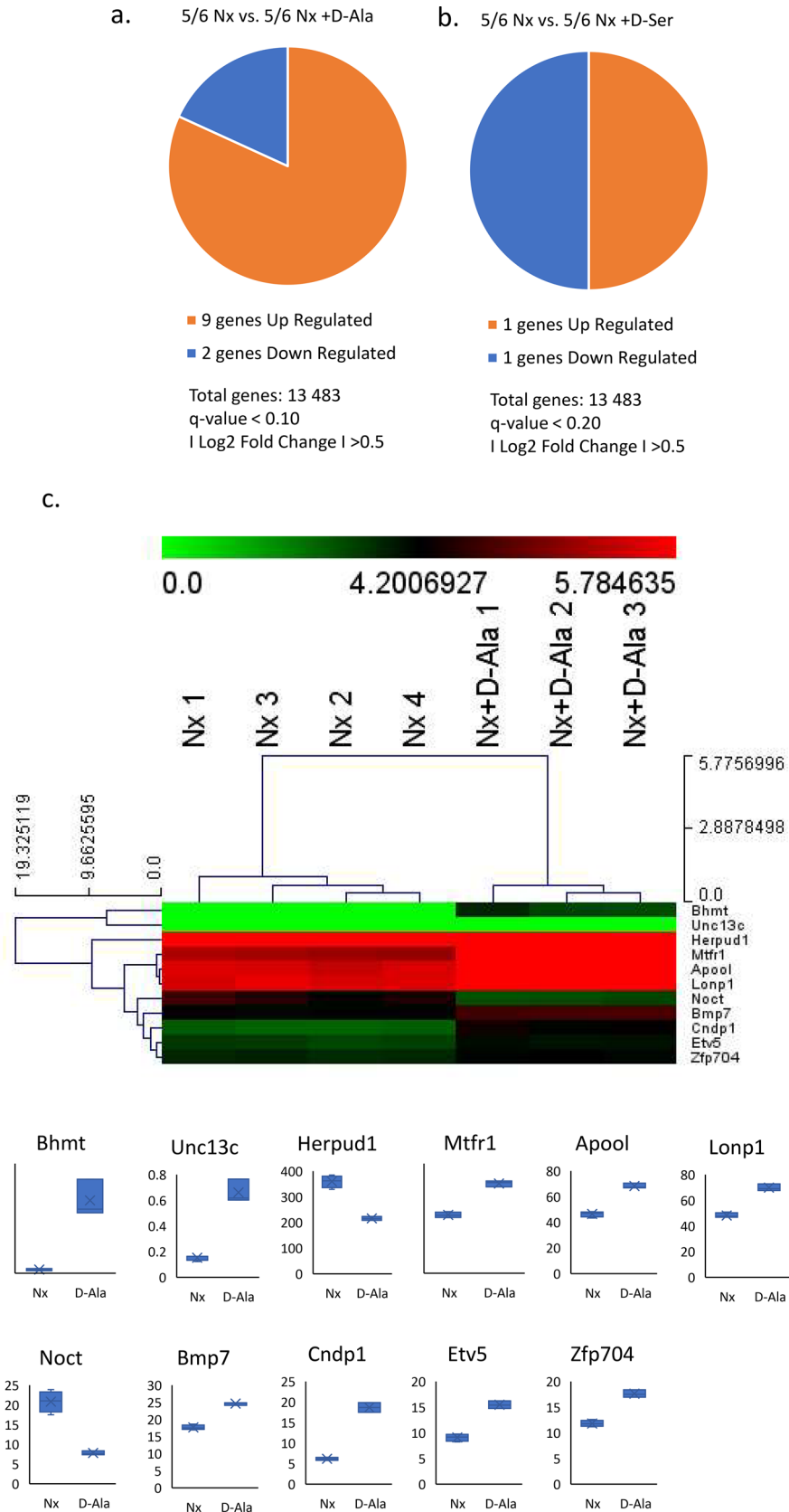


**Fig. 5.** RNA-Seq analysis of kidney tissues. Gene alteration in mice administered with D-Ala (a) and D-Ser (b) compared to mice administered with water. Heatmap (c) shows the differentially expressed genes between female 5/6-Nx mice and 20-mM D-Ala-treated female 5/6-Nx mice. Gene Ontology analysis (d) using 11 related female 5/6-Nx mice treated with 20 mM D-Ala. *D-Ala* D-alanine, *D-Ser* D-serine, *Nx* nephrectomy, *RNA-Seq* RNA-sequencing.

d.

Annotation Cluster 1: 1.9544540205493						
Category	Term	Count	%	PValue	List Total	Field Enrichment
BP_SCO_FEATURE	254077 Mitochondrion	4	38.4	0.001	11	16.36
BP_XW_DOMAIN	959 0001 Transmembrane	4	38.4	0.002	8	13.52
BP_XW_CELLULAR_COMPONENT	959 0006 Mitochondrion	4	38.4	0.027	11	5.26
DOTERM_BP_FAT	GO:0005747-mitochondrion organization	3	27.3	0.003	11	9.23
DOTERM_CC_FAT	GO:0000716-mitochondrion	4	38.4	0.004	10	3.33
Annotation Cluster 2: 0.73944202052029						
Category	Term	Count	%	PValue	List Total	Field Enrichment
DOTERM_MF_FAT	GO:0041403-transcription	7	63.6	0.028	9	2.18
DOTERM_MF_FAT	GO:0048752-transcription binding	5	45.5	0.005	9	2.38
DOTERM_MF_FAT	GO:0041910-catalytic binding	5	45.5	0.002	9	2.31
BP_XW_LIGAND	959 0002 DNA	4	38.4	0.009	6	1.88
BP_XW_LIGAND	959 0003 Transmembrane	5	45.5	0.005	6	1.45
BP_XW_CELLULAR_COMPONENT	959 0006 Mitochondrion	3	27.3	0.003	11	0.84
Annotation Cluster 3: 0.777962017018907						
Category	Term	Count	%	PValue	List Total	Field Enrichment
DOTERM_BP_FAT	GO:0042003-ribular macro-molecular catalytic process	3	27.3	0.100	11	0.69
DOTERM_BP_FAT	GO:0006057-macro-molecular catalytic process	3	27.3	0.144	11	4.03
DOTERM_BP_FAT	GO:0010101-response to organellar substance	4	38.4	0.002	11	1.62
Annotation Cluster 4: 0.84754010156019						
Category	Term	Count	%	PValue	List Total	Field Enrichment
DOTERM_MF_FAT	GO:0000710-regulatory region-DNA binding	3	27.3	0.142	9	3.05
DOTERM_MF_FAT	GO:0042423-transcription-regulatory region-DNA binding	4	27.3	0.162	9	2.69
DOTERM_MF_FAT	GO:0001067-regulatory region-nucleic acid binding	5	27.3	0.143	9	3.84
DOTERM_MF_FAT	GO:0042056-sequence-specific-DNA binding	3	27.3	0.198	9	3.57
BP_XW_MOLECULAR_FUNCTION	959 0008 DNA binding	3	27.3	0.162	9	3.23
DOTERM_MF_FAT	GO:0000716-nucleic acid binding	4	38.4	0.222	9	2.13
DOTERM_MF_FAT	GO:0000717-DNA binding	3	27.3	0.310	9	2.39
DOTERM_MF_FAT	GO:0010101-response to organellar substance	4	38.4	0.002	9	1.88
DOTERM_MF_FAT	GO:0001109-organic cyclic-compound binding	4	38.4	0.002	9	1.33
Annotation Cluster 5: 0.856439120473704						
Category	Term	Count	%	PValue	List Total	Field Enrichment
DOTERM_BP_FAT	GO:0006600-negative regulation of signal transduction	3	27.3	0.158	11	4.11
DOTERM_BP_FAT	GO:0010048-negative regulation of cell communication	3	27.3	0.167	11	3.88
DOTERM_BP_FAT	GO:0010207-negative regulation of signaling	3	27.3	0.167	11	3.67
DOTERM_BP_FAT	GO:0010208-negative regulation of cellular protein metabolic process	4	38.4	0.010	11	2.48
DOTERM_BP_FAT	GO:0010120-negative regulation of protein metabolic process	4	38.4	0.167	11	2.52
DOTERM_BP_FAT	GO:0040500-negative regulation of response to stimulus	3	27.3	0.229	11	3.00
DOTERM_BP_FAT	GO:0000000-protein binding	3	27.3	0.236	11	2.84
DOTERM_BP_FAT	GO:0010060-ribular response to chemical stimulus	4	38.4	0.268	11	2.91
DOTERM_BP_FAT	GO:0010100-negative regulation of protein modification process	3	27.3	0.270	11	2.68
DOTERM_BP_FAT	GO:0010048-negative regulation of cell communication	4	38.4	0.266	11	1.63
DOTERM_BP_FAT	GO:0010208-negative regulation of signaling	4	38.4	0.266	11	1.62
DOTERM_BP_FAT	GO:0006604-ribular protein modification process	4	38.4	0.320	11	1.83
DOTERM_BP_FAT	GO:0006211-protein modification process	4	38.4	0.320	11	1.62
DOTERM_BP_FAT	GO:0010101-response to organellar substance	4	38.4	0.320	11	1.63
DOTERM_BP_FAT	GO:0012110-ribular response to organic substance	3	27.3	0.442	11	1.86
DOTERM_BP_FAT	GO:0006600-negative regulation of signal transduction	3	27.3	0.483	11	1.73
Annotation Cluster 6: 0.872617610162003						
Category	Term	Count	%	PValue	List Total	Field Enrichment
DOTERM_BP_FAT	GO:0040422-ribular macro-molecular complex assembly	3	27.3	0.117	11	4.36
DOTERM_BP_FAT	GO:0010207-ribular component assembly	4	38.4	0.190	11	2.38
DOTERM_BP_FAT	GO:0005003-ribular macro-molecular complex assembly	3	27.3	0.214	11	2.83
DOTERM_BP_FAT	GO:0040500-ribular component biogenesis	4	38.4	0.220	11	2.16
DOTERM_BP_FAT	GO:0040303-macro-molecular complex subunit organization	3	27.3	0.259	11	2.76
DOTERM_BP_FAT	GO:0010100-response to organellar substance	3	27.3	0.262	11	2.68
DOTERM_BP_FAT	GO:0010101-response to organellar substance	4	38.4	0.320	11	1.82
DOTERM_BP_FAT	GO:0006780-phosphate containing compound metabolic process	3	27.3	0.503	11	1.67
DOTERM_BP_FAT	GO:0006710-phosphate metabolic process	3	27.3	0.518	11	1.63
Annotation Cluster 7: 0.907120010000001						
Category	Term	Count	%	PValue	List Total	Field Enrichment
DOTERM_BP_FAT	GO:0010207-ribular component assembly	4	38.4	0.190	11	2.38
DOTERM_BP_FAT	GO:0040500-ribular component biogenesis	3	27.3	0.260	11	2.88
DOTERM_BP_FAT	GO:0010048-negative regulation of cell communication	4	38.4	0.266	11	1.53
DOTERM_BP_FAT	GO:0010201-negative regulation of signaling	4	38.4	0.261	11	1.62
DOTERM_MF_FAT	GO:0041749-signal binding	3	27.3	0.401	9	1.68
Annotation Cluster 8: 0.93308140096072						
Category	Term	Count	%	PValue	List Total	Field Enrichment
DOTERM_BP_FAT	GO:0010141-ribular localization	4	38.4	0.200	11	2.31
DOTERM_BP_FAT	GO:0040500-ribular component biogenesis	3	27.3	0.260	11	2.88
DOTERM_BP_FAT	GO:0010048-negative regulation of cell communication	4	38.4	0.266	11	1.53
DOTERM_BP_FAT	GO:0010201-negative regulation of signaling	4	38.4	0.261	11	1.62
DOTERM_BP_FAT	GO:0010140-establishment of localization site	3	27.3	0.331	11	2.37
DOTERM_BP_FAT	GO:0005003-ribular macro-molecular complex assembly	3	27.3	0.427	11	1.68
Annotation Cluster 9: 0.948479610027336						
Category	Term	Count	%	PValue	List Total	Field Enrichment
DOTERM_BP_FAT	GO:0040501-positive regulation of cell differentiation	3	27.3	0.128	11	4.38
DOTERM_BP_FAT	GO:0010000-negative regulation of macro-molecular metabolic process	4	38.4	0.165	11	2.39
DOTERM_BP_FAT	GO:0010104-positive regulation of developmental process	3	27.3	0.216	11	5.12
DOTERM_BP_FAT	GO:0009000-negative regulation of metabolic process	4	38.4	0.217	11	2.22
DOTERM_BP_FAT	GO:0010020-negative regulation of gene expression	3	27.3	0.260	11	2.82
DOTERM_BP_FAT	GO:0040500-negative regulation of cell differentiation	3	27.3	0.308	11	2.45
DOTERM_BP_FAT	GO:0010020-negative regulation of gene expression	4	38.4	0.406	11	1.49
DOTERM_BP_FAT	GO:0010048-negative regulation of gene expression	4	38.4	0.406	11	1.44
DOTERM_BP_FAT	GO:0010481-gene expression	4	38.4	0.628	11	1.20
Annotation Cluster 10: 0.49330501104873						
Category	Term	Count	%	PValue	List Total	Field Enrichment
DOTERM_BP_FAT	GO:0010000-negative regulation of macro-molecular metabolic process	4	38.4	0.165	11	2.39
DOTERM_BP_FAT	GO:0010141-ribular localization	4	38.4	0.200	11	2.31
DOTERM_BP_FAT	GO:0009000-negative regulation of metabolic process	4	38.4	0.217	11	2.22
DOTERM_BP_FAT	GO:0010141-ribular localization	3	27.3	0.261	11	2.71
DOTERM_BP_FAT	GO:0010121-negative regulation of cellular metabolic process	3	27.3	0.442	11	1.86
DOTERM_BP_FAT	GO:0009000-negative regulation of metabolic process	4	38.4	0.266	11	2.51
DOTERM_BP_FAT	GO:0005003-ribular macro-molecular complex assembly	3	27.3	0.483	11	1.68
DOTERM_BP_FAT	GO:0010124-negative regulation of cellular metabolic process	3	27.3	0.442	11	1.86
DOTERM_BP_FAT	GO:0033000-macro-molecular localization	3	27.3	0.488	11	1.72
DOTERM_BP_FAT	GO:0010000-positive regulation of macro-molecular metabolic process	3	27.3	0.684	11	1.23
DOTERM_BP_FAT	GO:0010120-positive regulation of cellular metabolic process	3	27.3	0.571	11	1.64
DOTERM_BP_FAT	GO:0006600-positive regulation of metabolic process	3	27.3	0.620	11	1.37
Annotation Cluster 11: 0.33330704190396						
Category	Term	Count	%	PValue	List Total	Field Enrichment
DOTERM_MF_FAT	GO:0000716-nucleic acid binding	4	38.4	0.222	9	2.13
DOTERM_BP_FAT	GO:0014070-rRNA metabolic process	4	38.4	0.408	11	1.49
DOTERM_BP_FAT	GO:0010140-establishment of localization site	4	38.4	0.482	11	1.46
DOTERM_BP_FAT	GO:0010104-negative regulation of gene expression	4	38.4	0.260	11	1.38
DOTERM_MF_FAT	GO:0001109-organic cyclic-compound binding	4	38.4	0.532	9	1.33
BP_XW_CELLULAR_COMPONENT	959 0029 Nucleus	4	38.4	0.511	11	1.32
DOTERM_BP_FAT	GO:0010048-negative regulation of cell communication	4	38.4	0.628	11	1.29
Annotation Cluster 12: 0.2178181816200602						
Category	Term	Count	%	PValue	List Total	Field Enrichment
DOTERM_BP_FAT	GO:0008001-negative regulation of transcription from RNA polymerase II promoter	3	27.3	0.409	11	1.68
DOTERM_BP_FAT	GO:0010070-rRNA metabolic process	4	38.4	0.408	11	1.49
DOTERM_BP_FAT	GO:0010048-negative regulation of gene expression	4	38.4	0.482	11	1.44
DOTERM_BP_FAT	GO:0000710-transcription, DNA dependent	3	27.3	0.503	11	1.51
DOTERM_BP_FAT	GO:0008001-negative regulation of transcription, DNA dependent	3	27.3	0.589	11	1.44
DOTERM_BP_FAT	GO:0008000-negative regulation of nucleic acid templated transcription	3	27.3	0.589	11	1.44
DOTERM_BP_FAT	GO:0010141-negative regulation of RNA biophysical process	3	27.3	0.592	11	1.44
DOTERM_BP_FAT	GO:0009000-negative regulation of gene expression	3	27.3	0.684	11	1.48
DOTERM_BP_FAT	GO:0007174-rRNA biophysical process	3	27.3	0.613	11	1.39
DOTERM_BP_FAT	GO:0010481-gene expression	4	38.4	0.628	11	1.20
DOTERM_BP_FAT	GO:0010120-positive regulation of RNA metabolic process	3	27.3	0.684	11	1.48
DOTERM_BP_FAT	GO:0004854-nucleoside-containing compound biosynthetic process	3	27.3	0.673	11	1.38
DOTERM_BP_FAT	GO:0001112-negative regulation of cellular macro-molecular biosynthetic process	3	27.3	0.677	11	1.35
DOTERM_BP_FAT	GO:0010118-negative regulation of nucleoside-containing compound metabolic process	3	27.3	0.683	11	1.34
DOTERM_BP_FAT	GO:0010110-tetrapyclyc biophysical process	3	27.3	0.681	11	1.24
DOTERM_BP_FAT	GO:0010120-positive regulation of cellular macro-molecular biosynthetic process	3	27.3	0.684	11	1.48
DOTERM_BP_FAT	GO:0010000-negative regulation of macro-molecular biosynthetic process	3	27.3	0.685	11	1.23
DOTERM_BP_FAT	GO:0004841-ribular macro-molecular biophysical process	3	27.3	0.788	11	1.03

Fig. 5. (continued)

pathway<sup>24</sup>. Given that TGF-β/Smad3 activation is a major driver of CKD progression, our findings suggest that

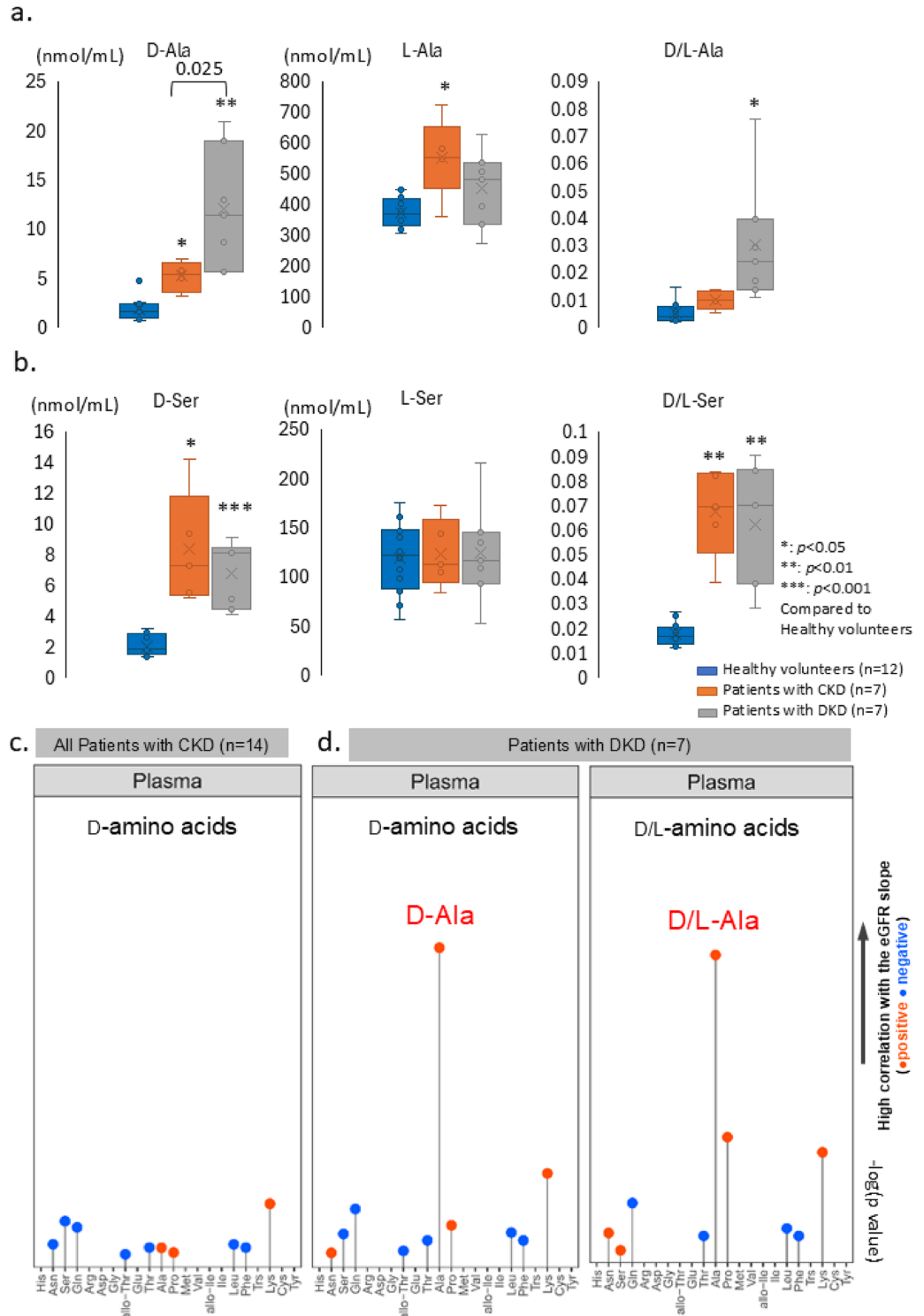


**Fig. 6.** Longitudinal study of associations between D-amino acids and kidney function. The plasma D-Ala (a) and D-Ser levels (b) of all patients with CKD. Box plots use horizontal lines to indicate the median, 25th, and 75th percentile values. D-Amino acid analysis of all patients with CKD (c). D-Amino acid and D/L-amino acid analysis in patients with DKD (d). The length of the bars indicates the statistical significance, and the color of the circles at the ends represents the direction of eGFR change associated with the amino acids, whether positive or negative. For example, in (c), the D-Ala bar shows a red circle at the end of a long bar, indicating that individuals with higher D-Ala levels had a significantly slower eGFR change ( $p < 0.0001$ ).  $*p < 0.05$ ,  $***p < 0.001$ , as analysed using one-way ANOVA. CKD chronic kidney disease, D-Ala D-alanine, DKD diabetic kidney disease, DM diabetes mellitus, D-Ser D-serine, D-Ala D-alanine, eGFR estimated glomerular filtration rate.  $*p < 0.05$ ,  $**p < 0.01$ ,  $***p < 0.001$ .

D-Ala-mediated *Bmp7* induction mitigates kidney injury by modulating fibrotic pathways. However, the precise molecular mechanisms underlying D-Ala-induced *Bmp7* upregulation remain unclear and require further investigation.

Interestingly, RNA-seq analysis also revealed increased *Cndp1* expression in D-Ala-treated mice. *Cndp1* encodes carnosinase-1, an enzyme that degrades carnosine, a dipeptide with antioxidant and anti-inflammatory properties. Previous studies suggest increased *Cndp1* activity may reduce renal protection by lowering carnosine levels, which contradicts our findings<sup>25–27</sup>. This discrepancy may stem from compensatory regulatory mechanisms or context-dependent effects of *Cndp1* expression in CKD. Further studies are needed to elucidate the functional significance of *Cndp1* upregulation in response to D-Ala treatment.

In contrast, D-Ser administration resulted in only minor changes in *Bhmt* and *Polr1a* expression. While D-Ser has been shown to promote TEC proliferation and tissue remodeling via the mTOR-related pathway<sup>10,11</sup>, its full effects may not be captured through transcriptomic analysis alone. Future studies integrating proteomic and metabolomic approaches may provide deeper insights into D-Ser's renoprotective mechanisms.

This study has several limitations. First, sex differences in survival rates were observed, with female 5/6-Nx mice exhibiting higher mortality than males. Future studies should evaluate the nephroprotective effects of D-Ser and D-Ala, specifically in male mice. Second, the systemic effects of these AAs on adipose tissue, muscle, and metabolic parameters were not extensively investigated. Third, the small patient cohort ( $n = 14$ ) had limited statistical power for robust conclusions. Larger, controlled clinical studies are needed to validate these findings.

In conclusion, D-Ser and D-Ala exhibited renoprotective effects in a severe CKD mouse model, likely through mitochondrial protection and inflammation reduction. D-Ala, in particular, may exert its effects via *Lonp1*-mediated mitochondrial protection, *Bmp7* induction, and NMDA receptor-mediated mitochondrial stabilization and ROS suppression<sup>12</sup>. The unexpected increase in *Cndp1* expression highlights the complexity of D-Ala's mechanisms and warrants further investigation. These findings underscore the therapeutic potential of D-Ala for CKD, necessitating further mechanistic and clinical studies.

## Methods

### Mice

The experimental groups included Sham + water, Nx + water, Nx + D-Ser, and Nx + D-Ala. Wild-type C57BL/6 mice (20 males and 20 females per group, totaling 160 mice) were purchased from CLEA (Osaka, Japan) and housed at Kanazawa University. All animal experiments were conducted following Kanazawa University's guidelines for animal care and were approved by the Institute for Experimental Animals, Kanazawa University (approval number: AP-204160). The experiments complied with the ARRIVE guidelines (<https://arriveguidelines.org>) (Supplementary Table 1). Mice were used for survival assessment, renal function evaluation, and renal tissue analysis. The final number of animals varied across experiments due to mortality, with exact numbers specified in the respective figures.

A combination of three anesthetic agents—medetomidine (Domitor), midazolam, and butorphanol (Vetorphale)—was used for anesthesia. The mixture was administered at a dose of 0.1 mL per 10 g of body weight via intraperitoneal injection. Upon completion of the procedure, a medetomidine antagonist solution was administered intraperitoneally at a dose of 0.1 mL per 10 g of body weight. Isoflurane inhalation was used for euthanasia.

D-Ser and D-Ala (Wako Co., Ltd., Tokyo, Japan) was orally administered at a concentration of 20 mM in distilled water. This concentration was selected based on previous studies demonstrating the nephroprotective effects of D-Ser at low concentrations (20 mM) and nephrotoxicity at higher concentrations (80 mM)<sup>10</sup>. For D-Ala, a concentration-dependent renoprotective effect was observed between 20 mM and 80 mM, with no nephrotoxic effects<sup>12</sup>. We used 20 mM for D-Ser and D-Ala to ensure safety and efficacy. Blood amino acid levels were measured on the first day following 5/6-Nx surgery. The mice's daily water and food intake was recorded over five days and averaged. Food and water intake was examined in additional mice. A graphical representation is shown in Supplemental Fig. 5a.

### 5/6-nephrectomy (Nx) CKD induction

Progressive renal failure was induced by 5/6 nephrectomy (5/6-Nx) through a two-step procedure in 6–8-week-old mice. All surgeries were performed under anesthesia. The upper and lower poles of the left kidney were severed using bipolar forceps (2/6-Nx). Liquid thrombin (Mochida Pharmaceutical Co. Ltd., Tokyo, Japan) was applied to the incision to prevent bleeding. Right kidney nephrectomy was performed after 2 weeks of recovery (5/6-Nx). The removal of the second kidney was designated as day 0. Sham surgery involved a two-step procedure in which the respective kidneys were exposed and repositioned.

### Sample collection and measurement

Urine was collected for 24 h in a mouse metabolic cage (SAN783No.2 A; Shinano Seisakusho Co., Ltd., Tokyo, Japan). Plasma BUN levels were measured using UN-S (Denka Co., Ltd., Tokyo, Japan). Plasma creatinine (Cr) levels were measured using a CRE·M (Wako, Co., Ltd., Osaka, Japan). Mouse blood pressure and heart rate were measured non-invasively using BP-98AL and BP98-MCFm (Softlon Co., Ltd., Taren Point, Australia). The mice were placed in a fixation device (ICN6; ICM Co., Ltd., Seoul, South Korea) to measure arterial pulse waves. An animal lancet (18310400, 5 mm; BRC Co., Ltd., Incheon, South Korea) was inserted into the mouse's sub-forehead vein to withdraw blood into ethylenediaminetetraacetic acid blood collection tubes (VP-DK053; Terumo Corp., Tokyo, Japan).

### Renal histopathology

Mouse kidneys were fixed in 10% formalin and embedded in paraffin. Paraffin sections were stained with periodic acid-Schiff (PAS) and azan. Kidney pathology was scored as previously described<sup>10,28</sup>. The PAS-stained debris at the corticomedullary junction, brush border, and cortical region were quantified in at least 10 kidney sections. Based on the proximal tubule dilation, brush border damage, presence of proteinaceous casts, interstitial widening, and necrosis, the acute tubular necrosis of the sections was scored and graded as follows: 0, none; 1, < 30%; 2, 30–60%; and 4, > 60% of the field.

### Hydroxyproline assay

Kidney fibrosis was evaluated using the hydroxyproline assay, as previously described<sup>10</sup>. The kidneys were assessed following the standard manufacturer's protocol. The results are expressed as micrograms ( $\mu\text{g}$ ) of hydroxyproline per 100 mg of kidney tissue.

### RNA-Sequencing (Seq) analysis

Total RNA was extracted from kidney samples of female 5/6-Nx mice or 20 mM D-Ser- or D-Ala-treated female 5/6-Nx mice ( $n = 4$  per group) using the NucleoSpin RNA Kit (Macherey-Nagel, Düren, Germany). The concentration and quality of the extracted RNA were measured using TapeStation and BioAnalyzer (Agilent Technologies, Santa Clara, CA, USA). Next, the cDNA libraries were prepared from RNAs using the SMART-Seq v4 Ultra Low Input RNA Kit for sequencing (Takara Bio, Tokyo, Japan) and the Nextera XT DNA Library Prep Kit (Illumina, San Diego, CA, USA) for RNA-Seq. RNA-Seq analysis was performed on a NovaSeq 6000 (Illumina) with a  $2 \times 150$  bp paired-end mode, providing an average of 69 million reads per sample. Finally, the RNA-Seq reads were mapped to the mouse genome (GRCm39), and gene-level expression was quantified (per gene read count) using the DRAGEN Bio-IT Platform (Illumina).

RNA-Seq of kidney samples from female 5/6-Nx mice were analyzed based on Benjamini–Hochberg-corrected  $p < 0.1$  and expression ratio  $> 1$ -fold ( $\log \text{FC} > 0.5$  or  $\log \text{FC} < -0.5$ ). A comparison of D-Ala-treated and untreated mice showed significant differences in genes based on Benjamini–Hochberg-corrected  $p < 0.1$  and expression ratio  $> 1$ -fold ( $\log \text{FC} > 0.5$  or  $\log \text{FC} < -0.5$ ). A comparison of D-Ser-treated and untreated mice showed no significant difference in genes based on Benjamini–Hochberg-corrected  $p < 0.1$  and expression ratio  $> 1$ -fold ( $\log \text{FC} > 0.5$  or  $\log \text{FC} < -0.5$ ). Therefore, the Benjamini–Hochberg-corrected  $p < 0.2$  and expression ratio  $> 1$ -fold ( $\log \text{FC} > 0.5$  or  $\log \text{FC} < -0.5$ ) were used.

Cluster analysis of genes was performed using MultiExperiment Viewer (<https://mev.tm4.org/#/about>). Then, GO enrichment analysis (Biological Process, Loves Park, IL, USA) was performed to estimate the function and subcellular localization of the D-Ser- or D-Ala-related genes using Database for Annotation, Visualization, and Integrated Discovery (<https://david.ncifcrf.gov/>)<sup>29,30</sup>.

### HK-2 cell proliferation assay

HK-2 cells (American Type Culture Collection, Manassas, VA, USA) were cultured in the recommended medium and maintained at 37 °C in a humidified chamber supplemented with 5% CO<sub>2</sub>. For the proliferation assay, cells were seeded in 96-well plates (4,000 cells/well) using Dulbecco's Modified Eagle Medium (DMEM) supplemented with 1% fetal bovine serum (FBS) and 1% penicillin–streptomycin. The next day, the culture medium was replaced with AA-free DMEM [048–33575] supplemented with MEM essential AAs [132–15641] and 100  $\mu\text{M}$  glycine [073–00732] and GlutaMax (L-Alanyl-L-Glutamine) [016–21841] (Fujifilm Wako, Tokyo, Japan) with 1% dialyzed FBS (26400–036, Gibco, Waltham, MA, USA), as previously described<sup>12</sup>. D-Ser or D-Ala was added to the culture medium after overnight incubation. After 1–2 days of culture, TEC proliferation was determined using Cell Counting Kit-8 (CK04; Dojindo, Tokyo, Japan), following the manufacturer's protocol. Live cells were detected by measuring the absorbance at 450 nm. Data are presented as the ratio of the sample optical density to the control optical density.

### Study population and sample collection

This prospective observational study included 14 patients with CKD. Their physical characteristics are shown in Table 1. This study investigated the association between increased blood D-Ser or D-Ala levels and long-term decline in renal function in these patients. The decline in renal function was evaluated using the estimated glomerular filtration rate (eGFR) slope. CKD was defined as an eGFR of  $\leq 60$  mL/min/1.73 m<sup>2</sup>. Patients treated with immunosuppressive drugs and antibiotics and those with suspected infectious diseases, body temperature  $> 37$  °C, diarrhea, or cancer were excluded. Blood samples were collected early in the morning from fasting participants. Immediately after collection, the samples were stored on ice, and plasma was separated by centrifugation and stored at  $-80$  °C until amino acid measurements were performed. Blood samples were collected from patients with CKD between 2013 and 2019 at Kanazawa University Hospital. A graphical representation of the process is shown in Supplemental Fig. 5b.

### Chiral AA determination using two-dimensional (2D) high-performance liquid chromatography (HPLC)

D- and L-AAs were evaluated using a 2D HPLC system (Nanospace SI-2 series; Shiseido, Tokyo, Japan), as previously described<sup>31,32</sup>. Briefly, 4-nitrobenzo-2-oxa-1,3-diazole (NBD)-AAs were isolated using an online fraction collecting system in the first dimension with a microbore-octadecyl silica column, prepared in a fused silica capillary (1,000  $\times$  0.53 mm i.d., 45 °C; Shiseido). The isolated fractions were automatically transferred to the second dimension comprising a narrow-bore enantio-selective column KSAACSP-001 S (250  $\times$  1.5 mm i.d., 25 °C; prepared in collaboration with Shiseido) to determine D- and L-enantiomers. The mobile phase used for

Characteristic	Healthy controls	All patients with CKD (n = 14)		p-value
		Patients with CKD	Patients with DKD	
N	12	7	7	
Sex (male, %)	100	42.9	85.7	
Age (years)	33.5 ± 13.5	61.1 ± 14.9	62.7 ± 12.6	<0.001
Height (cm)	171.0 ± 4.1	160.0 ± 10.5	161.6 ± 6.3	0.003
Weight (kg)	63.2 ± 7.8	63.5 ± 16.7	66.1 ± 14.4	0.882
Body mass index (kg/m <sup>2</sup> )	21.6 ± 2.4	24.7 ± 4.4	25.3 ± 5.7	0.113
Creatinine (mg/dL)	0.9 ± 0.1	2.7 ± 0.7	3.0 ± 1.5	0.017
eGFR (mL/min/1.73 m <sup>2</sup> )	81.7 ± 14.6	17.2 ± 4.3	21.3 ± 9.3	<0.001
Coronary artery disease (%)	0	0	0	
Stroke (%)	0	14	0	
Smoking habit (%)	8	100	71	
RAAS inhibitors use (%)	0	43	86	
SGLT2 inhibitors use (%)	0	0	0	
MRA use (%)	0	29	0	

**Table 1.** Clinical characteristics of the study participants. Values are presented as means ± standard deviations or %. *CKD* chronic kidney disease, *DKD* diabetic kidney disease, *eGFR* estimated glomerular filtration rate, *RAAS* Renin-angiotensin-aldosterone system, *SGLT* Sodium-glucose cotransporter 2, *MRA* Mineralocorticoid receptor antagonists.

the second dimension was a mixture of methanol and acetonitrile containing formic acid. Finally, fluorescence detection of NBD-AAs was conducted at 530 nm with excitation at 470 nm.

### Statistical analysis

Survival time analysis was performed using the Kaplan–Meier method. The t-test was used to test the differences between 5/6-Nx mice, healthy volunteers, and other mice or patients with CKD. Statistical significance was set at \* $p < 0.05$ , \*\* $p < 0.01$ , and \*\*\* $p < 0.001$ .

A mixed-effects model with a random intercept and slope was applied to calculate eGFR slopes during the study, using eGFR as the dependent variable and D-AA levels at baseline, time from baseline, and their multiplication terms as independent variables. The  $p$ -value was calculated to determine the association between the baseline AA levels and eGFR slopes.

Bonferroni correction was used to minimize type I errors because 22 AAs were tested for isomerism (type L, D, and D/L ratio). Statistical significance was set at a two-tailed  $p$ -value of 0.0001 (0.05/88).

### Data availability

The RNA-Seq analysis data (FASTQ reads) in this study have been deposited at the DNA Data Bank of Japan (DDBJ) under the DDBJ Sequence Read Archive (DRA) accession number, DRA016193.

Received: 19 April 2024; Accepted: 6 June 2025

Published online: 11 March 2026

### References

- Bikbov, B. et al. Global, regional, and National burden of chronic kidney disease, 1990–2017: a systematic analysis for the global burden of disease study 2017. *Lancet* **395**, 709–733 (2020).
- Ikizler, T. A. et al. KDOQI clinical practice guideline for nutrition in CKD: 2020 update. *Am. J. Kidney Dis.* **76**, S1–S107 (2020).
- Kalantar-Zadeh, K. & Fouque, D. Nutritional management of chronic kidney disease. *N Engl. J. Med.* **377**, 1765–1776 (2017).
- Mitch, W. E. & Remuzzi, G. Diets for patients with chronic kidney disease, should we reconsider? *BMC Nephrol.* **17**, 80 (2016).
- Wanner, C. et al. Empagliflozin and progression of kidney disease in type 2 diabetes. *N Engl. J. Med.* **375**, 323–334 (2016).
- Wiviott, S. D. et al. Dapagliflozin and cardiovascular outcomes in type 2 diabetes. *N Engl. J. Med.* **380**, 347–357 (2019).
- Perkovic, V. et al. Canagliflozin and renal outcomes in type 2 diabetes and nephropathy. *N Engl. J. Med.* **380**, 2295–2306 (2019).
- Chertow, G. M. et al. Effects of Dapagliflozin in stage 4 chronic kidney disease. *J. Am. Soc. Nephrol.* **32**, 2352–2361 (2021).
- Bakris, G. et al. Effects of Canagliflozin in patients with baseline eGFR < 30 ml/min per 1.73 m<sup>2</sup>: subgroup analysis of the randomized CREDENCE trial. *Clin. J. Am. Soc. Nephrol.* **15**, 1705–1714 (2020).
- Nakade, Y. et al. Gut microbiota-derived D-serine protects against acute kidney injury. *JCI Insight.* **3**, e97957 (2018).
- Hesaka, A. et al. d-Serine mediates cellular proliferation for kidney remodeling. *Kidney* **360**, 1611–1624 (2021).
- Iwata, Y. et al. Protective effect of d-alanine against acute kidney injury. *Am. J. Physiol. Ren. Physiol.* **322**, F667–F679 (2022).
- Nakade, Y. et al. Increased levels of oral Streptococcus-derived D-alanine in patients with chronic kidney disease and diabetes mellitus. *Sci. Rep.* **12**, 21773 (2022).
- Megumi, O. et al. Association between Risperidone use and kidney function decline in patients with schizophrenia: a retrospective cohort study. *Clin. Ther.* **45**, 889–893 (2023).
- Megumi, O. et al. Effects of D-alanine intake on amino acid metabolism in healthy adults: a multicenter, randomized pilot study. *Curr. Dev. Nutr.* **8**, 103787 (2024).
- Wen, C. P. et al. Diabetes with early kidney involvement May shorten life expectancy by 16 years. *Kidney Int.* **92**, 388–396 (2017).
- Gibellini, L. et al. The biology of Lonp1: more than a mitochondrial protease. *Int. Rev. Cell. Mol. Biol.* **354**, 1–61 (2020).

18. Bai, M. et al. LONP1 targets HMGCS2 to protect mitochondrial function and attenuate chronic kidney disease. *EMBO Mol. Med.* **15**, e16581 (2023).
19. Wenying, C. et al. Lonp1 and Sig-1R contribute to the counteraction of ursolic acid against Ochratoxin A-induced mitochondrial apoptosis. *Food Chem. Toxicol.* **172**, 113592 (2023).
20. Dudley, A. T., Lyons, K. M. & Robertson, E. J. A requirement for bone morphogenetic protein-7 during development of the mammalian kidney and eye. *Genes Dev.* **9**, 2795–2807 (1995).
21. Guld, S. E., Day, M., Jones, S. S. & Dorai, H. BMP-7 regulates chemokine, cytokine, and hemodynamic gene expression in proximal tubule cells. *Kidney Int.* **61**, 51–60 (2002).
22. Taro, T. et al. Roles and regulation of bone morphogenetic protein-7 in kidney development and diseases. *World J. Stem Cells.* **8**, 288–296. <https://doi.org/10.4252/wjsc.v8.i9.288> (2016).
23. Piscione, T. D., Phan, T. & Rosenblum, N. D. BMP7 controls collecting tubule cell proliferation and apoptosis via Smad1-dependent and -independent pathways. *Am. J. Physiol. Ren. Physiol.* **280**, F19–33 (2001).
24. Meng, X. M., Chung, A. C. & Lan, H. Y. Role of the TGF- $\beta$ /BMP-7/Smad pathways in renal diseases. *Clin. Sci. (Lond.)* **124**, 243–254 (2013).
25. Ahluwalia, T. S., Lindholm, E. & Groop, L. C. Common variants in CNBP1 and CNBP2, and risk of nephropathy in type 2 diabetes. *Diabetologia* **54**, 2295–2302 (2011).
26. Tziastoudi, M., Stefanidis, I. & Zintzaras, E. The genetic map of diabetic nephropathy: evidence from a systematic review and meta-analysis of genetic association studies. *Clin. Kidney J.* **13**, 768–781 (2020).
27. Weigand, T. et al. A global Cndp1-knock-out selectively increases renal carnosine and Anserine concentrations in an age- and gender-specific manner in mice. *Int. J. Mol. Sci.* **21**, 4887 (2020).
28. Iwata, Y. et al. Involvement of CD11b+GR-1 low cells in autoimmune disorder in MRL-Fas Lpr mouse. *Clin. Exp. Nephrol.* **14**, 411–417 (2010).
29. Huang da, W., Sherman, B. T. & Lempicki, R. A. Systematic and integrative analysis of large gene lists using DAVID bioinformatics resources. *Nat. Protoc.* **4**, 44–57 (2009).
30. Huang da, W., Sherman, B. T. & Lempicki, R. A. Bioinformatics enrichment tools: paths toward the comprehensive functional analysis of large gene lists. *Nucleic Acids Res.* **37**, 1–13 (2009).
31. Koga, R. et al. Enantioselective two-dimensional high-performance liquid chromatographic determination of N-methyl-D-aspartic acid and its analogues in mammals and bivalves. *J. Chromatogr. A.* **1269**, 255–261 (2012).
32. Hamase, K. et al. Simultaneous determination of hydrophilic amino acid enantiomers in mammalian tissues and physiological fluids applying a fully automated micro-two-dimensional high-performance liquid chromatographic concept. *J. Chromatogr. A.* **1217**, 1056–1062 (2010).

## Acknowledgements

We thank the staff for their technical support and Ms. Yuko Oyama and Ms. Mari Shimizu for mouse breeding management, and Ms. M. Nakane and the staff of KAGAMI Co., Ltd. for their technical support in two-dimensional high-performance liquid chromatography (2D-HPLC) and biostatistical analyses. We would like to thank Editage ([www.editage.com](http://www.editage.com)) for editing the English language.

## Author contributions

Conceived and designed the experiments: Yusuke Nakade, Yasunori Iwata, Megumi Oshima, Toshiaki Tokumaru, Shinji Kitajima, Miho Shimizu, Norihiko Sakai, and Takashi Wada. Performed the experiments: Yusuke Nakade and Taku Kobayashi. Analysed the data: Yusuke Nakade, Yuta Yamamura, and Tadashi Toyama. Contributed materials/analysis tools: Masashi Mita. Wrote the paper: Yusuke Nakade, Yasunori Iwata, and Takashi Wada.

## Funding

This research was supported by Grants-in-Aid from the Ministry of Education, Culture, Sports, Science, and Technology of the Japanese Government under Grant Numbers 17K08978 and 21K07315 (Y.N.) and AMED under Grant Number JP21ek0310012 (T.W.).

## Declarations

## Competing interests

The authors declare no competing interests.

## Ethical approval

This study was approved by the Ethics Committee of Kanazawa University Hospital (IRB approval no. 1291) and followed the principles of the Declaration of Helsinki. Written informed consent was obtained from all participants.

## Additional information

**Supplementary Information** The online version contains supplementary material available at <https://doi.org/10.1038/s41598-025-06251-y>.

**Correspondence** and requests for materials should be addressed to Y.I.

**Reprints and permissions information** is available at [www.nature.com/reprints](http://www.nature.com/reprints).

**Publisher's note** Springer Nature remains neutral with regard to jurisdictional claims in published maps and institutional affiliations.

**Open Access** This article is licensed under a Creative Commons Attribution-NonCommercial-NoDerivatives 4.0 International License, which permits any non-commercial use, sharing, distribution and reproduction in any medium or format, as long as you give appropriate credit to the original author(s) and the source, provide a link to the Creative Commons licence, and indicate if you modified the licensed material. You do not have permission under this licence to share adapted material derived from this article or parts of it. The images or other third party material in this article are included in the article's Creative Commons licence, unless indicated otherwise in a credit line to the material. If material is not included in the article's Creative Commons licence and your intended use is not permitted by statutory regulation or exceeds the permitted use, you will need to obtain permission directly from the copyright holder. To view a copy of this licence, visit <http://creativecommons.org/licenses/by-nc-nd/4.0/>.

© The Author(s) 2026